JPEDAV (2011) 32:97–104
DOI: 10.1007/s11669-010-9808-3
1547-7037 ©ASM International

Phase Equilibria in the Fe-Nb System

S. Voß, M. Palm, F. Stein, and D. Raabe

(Submitted September 8, 2010)

A review of the literature revealed that recently published phase diagrams of the Fe-Nb system show considerable discrepancies regarding phase equilibria with the melt and the homogeneity ranges of the intermetallic phases, specifically of the Laves phase Fe_2Nb. Therefore the system has been reinvestigated by metallography, electron probe microanalysis (EPMA), and differential thermal analysis (DTA). Temperatures of invariant reactions were determined and the homogeneity ranges of the two intermetallic phases, Fe_2Nb Laves phase and Fe_7Nb_6 μ phase, which both exist within a wide composition range, were established.

Keywords binary system, experimental study, intermetallics, phase diagram

1. Introduction

The Fe-Nb system is of high interest as Nb is an essential alloying element for steels. It is known since long that Nb acts in a wide variety of steels and Fe-containing alloys for ambient and high temperatures in multiple ways, e.g. through solid solution, micro-carbide formation, and the formation of intermetallic phases [1938Egg, 1938Vog, 1939Gen, 1942Wev]. Particularly the latter aspect recently attracts increasing attention as alloys that are strengthened by fine precipitates of the Laves phase Fe_2Nb offer considerable strength and creep resistance also at elevated temperatures [2002Kne, 2005Fal, 2008Yam]. A first comprehensive Fe-Nb phase diagram, presented by Goldschmidt [1957Gol, 1960Gol], showed four intermetallic phases denoted as ρ (Laves phase Fe_2Nb), σ ($Fe_{21}Nb_{19}$), $\bar{\eta}$ (Fe_3Nb_2) and μ, a possible high temperature phase at 90 at.% Nb. However, the phase diagram by Paul and Swartzendruber [1986Pau] which was assessed on the basis of all data available up to 1983, shows only two intermetallic phases, namely the hexagonal C14-type Laves phase Fe_2Nb (now denoted as ε) and Fe_7Nb_6 (μ phase). The latter is identical to the σ phase proposed by Goldschmidt [1960Gol], while the $\bar{\eta}$ phase was identified to be of Ti_2Ni-type, a phase which is stabilized by interstitial impurities [1967Ram, 1968Kri, 1985Lue, 1991Zel, 1996Sch]. The assessment by Paul and Swartzendruber [1986Pau] was also the basis for the updates by Okamoto [1993Oka, 1995Oka, 2002Oka] and his most recent version of the Fe-Nb system is shown in Fig. 1. Actually this is an overlay of two diagrams which have been assessed by Srikanth and Petric [1994Sri] (dashed lines) and Toffolon and Servant [2000Tof] (solid lines). The fact, that two phase diagrams which differ considerably from each other are reproduced in the most recent assessment already indicates the uncertainties that still exist about phase equilibria in the Fe-Nb system. The two superimposed diagrams agree in that besides the two solid solutions only two intermetallic phases exist in the system. The Laves phase Fe_2Nb forms congruently at about 1640 °C while the μ phase Fe_7Nb_6 forms peritectically—not congruently as indicated in some previous reports—by the invariant reaction $Fe_7Nb_6 \leftrightarrow L + Fe_2Nb$ at about 1520 °C. However, there is a striking difference in the homogeneity ranges for the two intermetallic phases (Fig. 1). The homogeneity ranges for the Laves phase Fe_2Nb hardly overlap at all in the two diagrams and while the assessment of [1994Sri] indicates that Fe_7Nb_6 is a line compound of fixed composition the phase has an extended homogeneity range according to [2000Tof] which in addition shifts with temperature. Even Okamoto [2002Oka] seems not to be sure which diagram is more valid. While he claims that the assessment by Toffolon and Servant [2000Tof] better fits the experimental data, all temperatures shown in his assessment are actually those of Srikanth and Petric [1994Sri] (Fig. 1). It is noted that a number of additional thermodynamic assessments exists [1975Kau, 1990Hua, 2008Yos], but these failed to reproduce phase diagrams in accordance with the experimental evidence as discussed below.

Recently, the homogeneity range of the Laves phase Fe_2Nb has been determined at 1100 °C [2007Gru] and at 1200 °C [2005Tak] by electron probe microanalysis (EPMA) on quenched samples and in their interdiffusion study [2010Bal] detected the Laves phase by EDS analysis of diffusion couples heat-treated between 950 and 1200 °C at 28-37 at.% Nb. These investigations show that at least at these temperatures the homogeneity range is much wider then indicated in [1994Sri, 2000Tof].

Within the framework of the large-scale research initiative "The Nature of Laves Phases" (http://laves.mpie.de) the authors aim at determining the basic mechanical behaviour of Laves phases which has not been well established yet. To this end, single-phase material of a number of Laves phases had to be produced [2010Vos]. Because first trials to produce single-phase Fe_2Nb revealed that none of the present phase diagrams shows the correct homogeneity range for this phase, the Fe-Nb system has been reinvestigated.

S. Voß, M. Palm, F. Stein, and **D. Raabe**, Max-Planck-Institut für Eisenforschung GmbH, Max-Planck-Str. 1, 40237 Düsseldorf, Germany. Contact e-mail: s.voss@mpie.de.

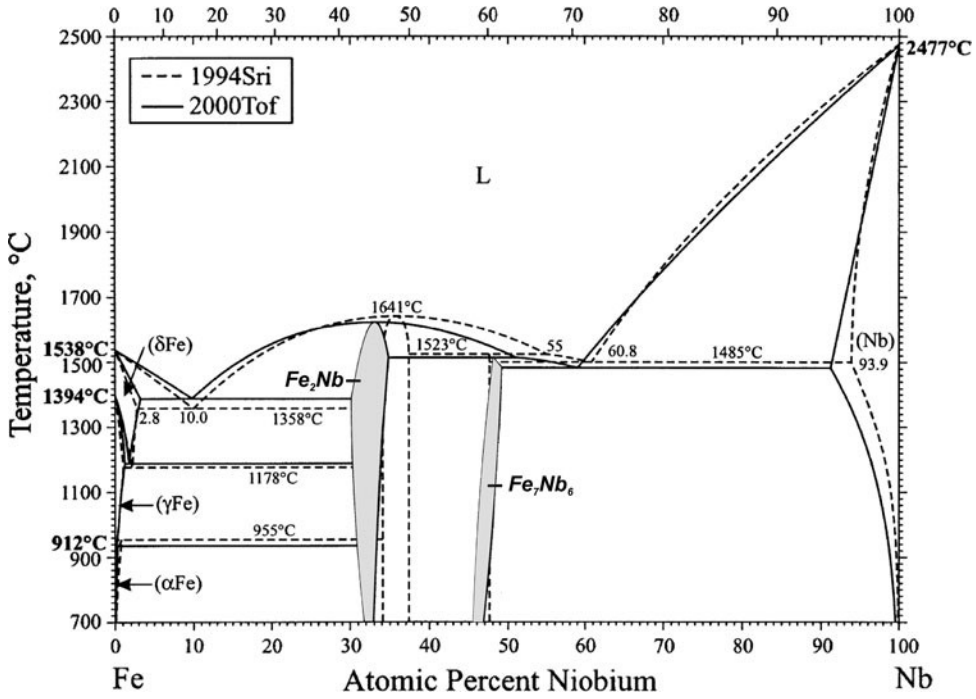

Fig. 1 Recent assessment of the Fe-Nb system [2002Oka], which is an overlay of the thermodynamic assessments by Toffolon and Servant [2000Tof] (solid lines and shaded areas) and Srikanth and Petric [1994Sri] (dashed lines and temperatures)

2. Experimental Procedure

Three alloys of up to 350 g were prepared by arc-melting from Fe with 99.95 wt.% purity (electrolytic Fe (TOHO ZINC Co., Ltd.) remolten by vacuum induction melting to reduce the O content) and Nb with 99.9 wt.% purity (GfE Metalle und Materialien GmbH). The amounts of non-metallic impurities were determined by carrier gas hot extraction. 13 single-phase Laves phase alloys were produced by a modified levitation melting method described in detail in [2010Vos]. For both melting processes, the vessel was evacuated and refilled with Ar (purity 99.999 wt.%) for several times and melting and casting were performed in a static Ar inert gas atmosphere. Typical impurity contents are 100-300 wt. ppm O, 40-75 wt. ppm C, and <10 wt. ppm N [2010Vos]. In addition, one diffusion couple was prepared by putting rectangular pieces of the pure elements of dimensions $5 \times 5 \times 8$ mm^3 with ground surfaces onto each other and wrapping them into a Ta foil.

Heat-treatments were carried out at temperatures between 1000 and 1450 °C for up to 1000 h. For heat treatments at 1000 and 1150 °C samples were encapsulated in evacuated quartz ampoules backfilled with Ar which were quenched in brine. Samples heat-treated at 1300 and 1450 °C were wrapped in Ta foil, put in an alumina crucible and covered with Ti filings for prevention of oxidation. Heat treatments were performed in a dynamic Ar inert gas atmosphere with subsequent cooling in a cold Ar jet. Only the diffusion couple was cooled down with 10 K/min in the furnace to prevent the intermetallic phase zones from disintegration.

Melting temperatures and phase transformations were established by differential thermal analysis (DTA) using a Setaram SETSYS-18 DTA. The samples were placed in alumina crucibles and measured under an Ar inert gas atmosphere with a heating/cooling rate of 5 or, in a few cases, 1, 10 or 20 K/min. Solidus and liquidus temperatures were determined according to the standard procedures recommended by Böttinger et al. [2006Boe, 2007Boe].

For light optical and scanning electron microscopy (LOM, SEM) samples were cut by electrical discharge machining (EDM), embedded in epoxy resin and mechanically polished down to 1 μm and etched with "Ti2" (68% glycerine, 16% HNO_3 and 16% HF). For determining the compositions of the phases and to check the chemical homogeneity of the single-phase samples, EPMA was carried out on a Jeol JXA 8100. Some samples were analyzed by energy-dispersive spectrometry (EDS) using a Hitachi S-530 scanning electron microscope (SEM) equipped with a CDU-LEAP system from EDAX. While compositions of phases were measured with a spot size of 1 μm, the beam was widened to 10-20 μm for the determination of the fine-scaled eutectics. Overall compositions of the alloys were established by measuring at least two grids of 25×25 points with 10 μm step size and 1 μm spot size and averaging the results. The concentration profile of the diffusion couple was established by measuring several line scans with a step size of 1 μm and 1 μm spot size along the diffusion path. Compositions of coexisting phases were established by extrapolating the measured concentration profile onto the phase boundary [1994Kai]. For the

determination of the eutectoid area the spot size was increased to 5 µm. Because fine precipitates of Fe_2Nb formed during cooling in δFe, a spot size of 20 µm and a step size of 5 µm were employed for the determination of the composition of δFe at the γFe/δFe interface.

3. Results and Discussion

Table 1 lists the compositions of the phases determined by EPMA and Table 2 shows temperatures recorded by DTA. The phase diagram established from these data is presented in Fig. 2. The melting temperatures of the pure metals as well as the temperature of the γ/δ transformation in pure Fe are taken from [2002Oka]. In addition, EPMA [1991Zel, 1993bZel, 2005Tak, 2007Gru] and DTA [1993bZel] data are shown from the most recent investigations of the Fe-Nb system. These results are in good agreement with the present data.

3.1 Liquidus

Figure 3 shows the as-cast microstructures of the three two-phase alloys. The alloys with 13.5 and 57.6 at.% Nb show large areas with eutectic microstructure, which allows the determination of the overall composition of the eutectic, which resembles that of the liquid at the eutectic reaction, by EPMA by measuring with a widened beam. The microstructure of the alloy with 13.5 at.% Nb (Fig. 3a) contains primary Laves phase in addition to the eutectic, which already indicates that the composition of the eutectic must be at a somewhat lower Nb content than the composition of this alloy. By EPMA the composition of the liquid at the eutectic L ↔ δFe + Fe_2Nb was determined as 8.2 ± 0.7 at.% (the compositions of all phases at the invariant reactions are given in Table 3). This measured composition is somewhat lower than previously evaluated data of 9.8 [1937Vor], 11.3-11.7 [1938Egg], 13.8 [1938Vog], 10.6 [1961Gib], 12 ± 0.2 at.% Nb [1964Fer] and than assessed data, i.e. 10.6 [1982Kub], 12.1 [1986Pau], 10.0 [1994Sri, 1995Oka, 2000Tof, 2002Oka], and

Table 1 Analysed compositions of alloys, heat treatments, and compositions of phases and homogeneity ranges obtained from the samples and the diffusion couple (DC) by EPMA

Analysed composition, at.% Nb	Heat treatment, °C/h	Composition of phases, at.% Nb			
		Fe	Fe_2Nb	Fe_7Nb_6	Nb
13.5	1300/100	…(a)	26.2 ± 0.2		
13.5	1150/500	…(a)	27.0 ± 0.3		
13.5	1000/1000	…(a)	27.6 ± 0.3		
26.4	As-cast		27.2(b)		
29.7	1350/50		29.7		
29.8	As-cast		29.8(c)		
31.0	As-cast		31.0(c)		
31.6	As-cast		31.6		
31.8	As-cast		31.8		
32.9	As-cast		32.9		
33.0	As-cast		33.0(c)		
33.6	As-cast		33.6		
33.9	As-cast		33.9(c)		
34.4	1350/50		34.4		
35.0	As-cast		35.0(d)		
35.1	As-cast		35.1(c),(d)		
38.6	1450/10		36.3 ± 0.3	46.9 ± 0.3	
38.6	1300/100		35.2 ± 0.4	46.5 ± 0.3	
38.6	1150/500(e),(f)		34.3 ± 0.3	46.3 ± 0.5	
38.6	1000/1000		34.8 ± 0.5	46.9 ± 0.3	
57.6	1450/10			50.4 ± 0.3	91.4 ± 0.1
57.6	1300/100			50.0 ± 0.3	93.4 ± 0.3
57.6	1150/500(f),(g)			49.6 ± 0.6	95.0 ± 0.4
57.6	1000/1000			48.3 ± 0.3	95.7 ± 0.4
DC Fe/Nb	1300/240	0-0.8 (γFe) 1.2-1.7 (δFe)	26.4-34.8	46.3-49.6	94.2-100

(a) No equilibrium composition measurable because of transformations during quenching. (b) Contains traces of Fe. (c) Composition measured by EDS instead of EPMA. (d) Contains traces of Fe_7Nb_6. (e) Contains a small amount of an additional phase, possibly with Ti_2Ni structure according to [2007Gru]. (f) Additional phases presumably formed due to impurities stemming from a loss in gas-tightness of the quartz ampoules. According to the data established at higher and lower temperatures, it is assumed that they did not markedly affect the phase equilibria. (g) Contains a small amount of NbC

Table 2 Solidus and liquidus temperatures determined by DTA with a heating/cooling rate of 5 (*: 10) K/min

Analysed composition, at.% Nb	Heat treatment, °C/h	Temperatures recorded by DTA, °C				
		$T_{Curie}(\alpha Fe)$	$T_{\alpha Fe \leftrightarrow \gamma Fe}$	$T_{\gamma Fe \leftrightarrow \delta Fe}$	$T_{Solidus}$	$T_{Liquidus}$
13.5	As-cast	769 ± 1	943 ± 25	1183 ± 15	1373 ± 1	1465 ± 3
26.4	As-cast				1367 ± 1	1626 ± 3
29.7	1350/50				1575 ± 5	1640 ± 3
29.8	As-cast				1577 ± 5	1634 ± 3
31.0	As-cast				1585 ± 5	1633 ± 3
31.6	As-cast				1620 ± 3	1644 ± 3
31.8	As-cast				1614 ± 3	1645 ± 3
32.9	As-cast				1631 ± 5*	1633 ± 5*
33.0	As-cast				1634 ± 5*	1642 ± 5*
33.6	As-cast				1630 ± 3	1645 ± 3
33.9	As-cast				1628 ± 3	1643 ± 3*
34.4	1350/50				1613 ± 3	1647 ± 3
35.0	As-cast				1605 ± 3	1640 ± 3
35.1	As-cast				1596 ± 5	1638 ± 3*
38.6	As-cast				1523 ± 2	1633 ± 3
57.6	1450/10				1508 ± 2	1509 ± 3

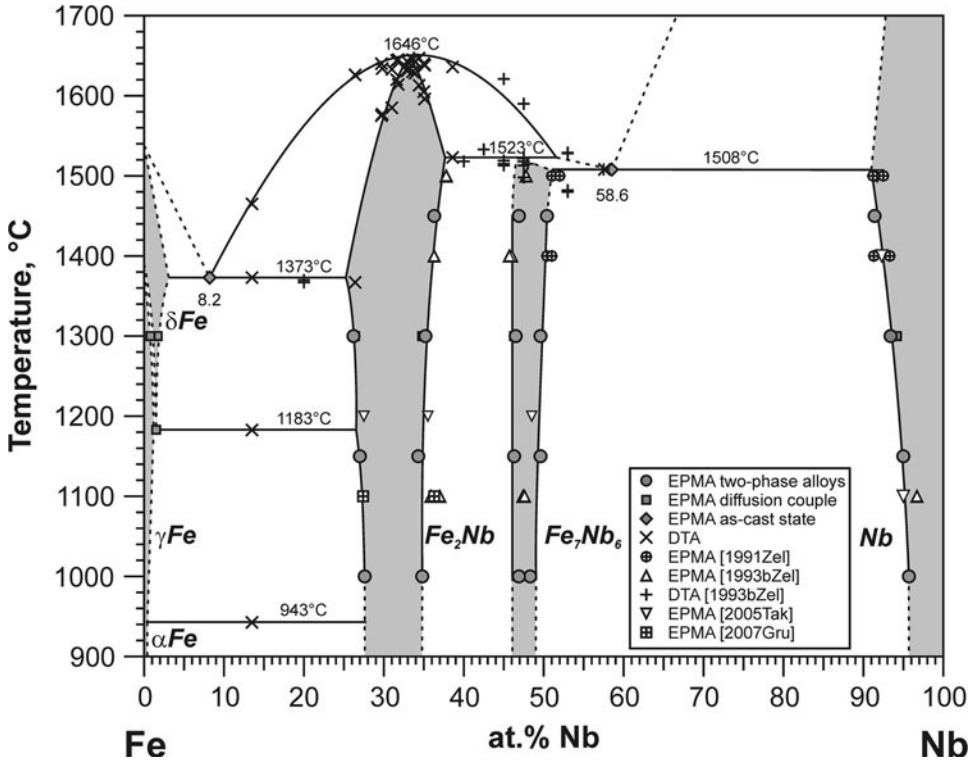

Fig. 2 The Fe-Nb phase diagram as established from EPMA or EDS measurements on equilibrated samples, the diffusion couple, as-cast alloys (eutectic compositions), and from DTA with additional EPMA and DTA data from literature

12.1 at.% Nb [1993Oka]. However, the only available measurement of the eutectic also indicates a lower Nb content of ~10 at.% Nb [1971aLei]. The temperature of 1373 ± 1 °C for the invariant reaction L ↔ δFe + Fe_2Nb measured by DTA is in excellent agreement with previous data: 1365 °C [1937Vor], 1372 ± 2 °C [1961Gib], 1370 ± 1 °C [1964Fer], 1367 ± 15 °C [1972Bew], 1370 °C [1993bZel], but somewhat higher than 1356 °C [1938Egg] and 1360 °C [1938Vog].

Figure 3(c) shows that the as-cast microstructure of the alloy with 57.6 at.% Nb is nearly fully eutectic and the measured composition of the eutectic of 58.6 ± 0.5 at.% for

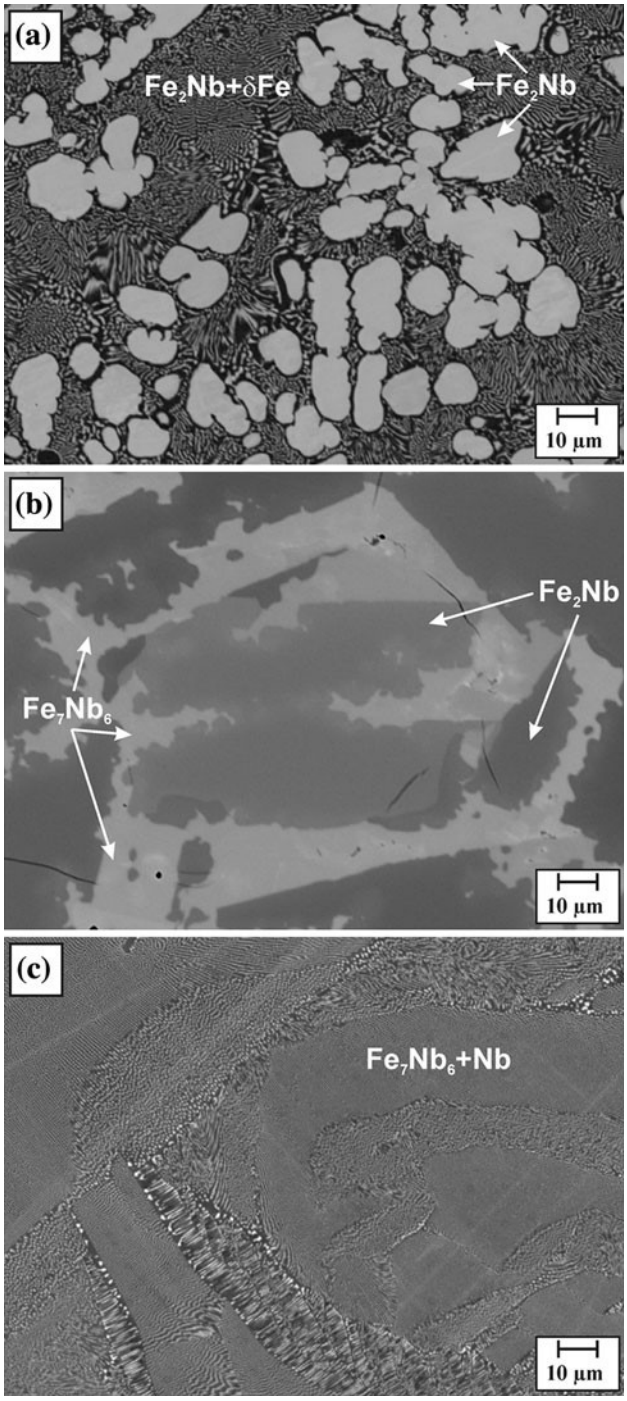

Fig. 3 SEM micrographs (backscattered-electron (BSE) contrast) of the as-cast microstructures of the three two-phase alloys: (a) 13.5 at.% Nb, primary Laves phase Fe_2Nb (light) and fine-scaled δFe + Fe_2Nb eutectic; (b) 38.6 at.% Nb, primary Laves phase Fe_2Nb (grey; different grey scales originate from different crystallographic orientations of the grains) surrounded by peritectically formed Fe_7Nb_6 (light); (c) 57.6 at.% Nb, nearly fully eutectic Nb + Fe_7Nb_6

$L \leftrightarrow Fe_7Nb_6 + Nb$ is close to that of the alloy. The composition of the eutectic has not been measured before. Data evaluated from the course of the liquidus lines scattered considerably, e.g. 55-55.5 at.% Nb [1938Egg], 61.9 at.% Nb [1938Vog], 59 at.% Nb [1993bZel] and assessed data indicated an even higher Nb content for the eutectic, e.g. 59-66 at.% Nb [1975Kau, 1986Pau, 1990Hua, 1993Oka, 1994Sri, 1995Oka, 2000Tof, 2002Oka, 2008Yos], but it is noted that these assessments were based on a rather limited amount of data. The eutectic temperature of 1508 ± 2 °C measured by DTA is within the range of previous data which however scatter considerably: 1560 °C [1938Egg], 1515 °C [1938Vog], ~ 1500 °C [1991Zel]. In addition a temperature of 1507 ± 20 [1972Bew] has been reported, but it had been attributed to a eutectic between Fe_2Nb and Fe_7Nb_6 which apparently does not exist.

Table 3 Temperatures of invariant reactions (DTA) and their respective phase compositions

Invariant reaction	Temperature, °C	Respective phase compositions, at.% Nb		
$Fe_2Nb + L \leftrightarrow Fe_7Nb_6$	1523 ± 2	37.6	~52	46.5
$L \leftrightarrow Fe_7Nb_6 + Nb$	1508 ± 2	**58.6 ± 0.5**	51.0	91.0
$L \leftrightarrow \delta Fe + Fe_2Nb$	1373 ± 1	**8.2 ± 0.7**	3.2	25.1
$\delta Fe \leftrightarrow \gamma Fe + Fe_2Nb$	1183 ± 15*	**1.5 ± 0.1**	1.1	26.5
$\gamma Fe + Fe_2Nb \leftrightarrow \alpha Fe$	943 ± 25*	n.d.	27.6	n.d.

Compositions given in bold are measured by EPMA. All other data are established from the extrapolation shown in Fig. 2
DTA: heating rate 5 K/min, except *: 1 K/min
n.d.: not determined

Figure 3(b) shows the as-cast microstructure of the alloy with 38.6 at.% Nb, which consists of primary Fe_2Nb surrounded by Fe_7Nb_6 that has formed by the peritectic reaction $L + Fe_2Nb \leftrightarrow Fe_7Nb_6$. This observation confirms that Fe_7Nb_6 does not melt congruently as claimed in some previous reports [1967Ram, 1972Bew, 1982Kub, 1990Hua]. The temperature for the peritectic reaction of 1523 ± 2 °C fits well with the only one previously measured temperature of 1520 °C [1993bZel].

3.2 Fe-Rich Part

In the Fe-rich portion of the phase diagram the temperatures of the invariant reactions $\gamma Fe + Fe_2Nb \leftrightarrow \alpha Fe$ and $\delta Fe \leftrightarrow \gamma Fe + Fe_2Nb$, the solid solubility of Nb in δFe at 1300 °C, the eutectoid composition (composition of δFe) and the ferromagnetic Curie temperature of αFe have been determined.

DTA experiments performed with heating/cooling rates of 1, 5, 10, and 20 K/min reveal that the onset temperatures of the two invariant reactions strongly depend on the applied heating and cooling rate. The two values given below are the average temperatures obtained from experiments at 1 K/min. The temperature for the peritectoid reaction $\gamma Fe + Fe_2Nb \leftrightarrow \alpha Fe$ is determined by DTA as 943 ± 25 °C, which is somewhat lower than previously published data: 965 °C [1938Egg], 989 °C [1939Gen], 960 °C [1970Fis]. Due to this reaction the composition of γFe could not be determined in the alloy with 13.5 at.% Nb after quenching (Table 1). The eutectoid

reaction δFe ↔ γFe + Fe_2Nb takes place at 1183 ± 15 °C, which is again slightly lower than previously reported data: 1220 °C [1938Egg], 1220 °C [1939Gen], 1200 °C [1961Gib], 1208 °C [1964Fer], 1190 °C [1970Fis]. The composition of the eutectoid was measured by EPMA with a widened beam (5 µm spot size) in the diffusion couple (Fig. 4). The obtained value of 1.5 ± 0.1 at.% Nb is in perfect agreement with previous extrapolated data [1939Gen, 1964Fer, 1970Fis], with the exception of [1961Gib] who found 2.8 at% Nb. From the diffusion couple the equilibrium compositions at 1300 °C of γFe (0.8 at.% Nb) and δFe (1.2-1.7 at.% Nb) were also determined. Because Laves phase precipitates formed during cooling in former δFe, the composition of the Nb-rich phase boundary of δFe was determined by extrapolating the diffusion profiles—which were measured with a widened beam using a spot size of 20 µm and 5 µm step size—onto the phase boundary. For the ferromagnetic Curie temperature of αFe a value of 769 ± 1 °C was measured by DTA, very well agreeing with the data of Eggers and Peters [1938Egg] who determined 768 ± 3 °C, i.e. the Curie temperature of pure Fe is not affected by the addition of Nb within the experimental accuracy. Figure 5 summarises the results in the Fe-rich part.

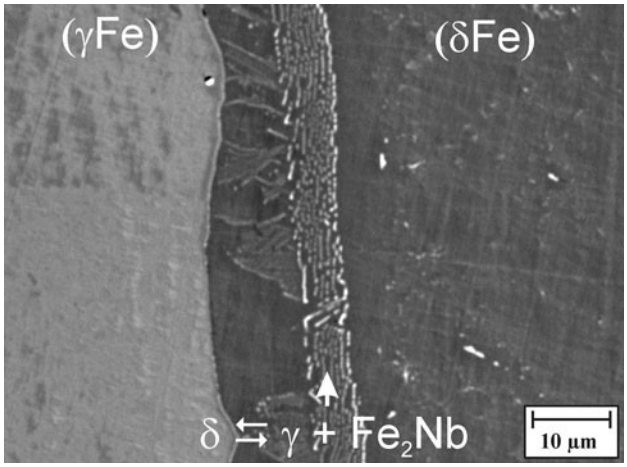

Fig. 4 SEM micrograph (BSE contrast) of the Fe-rich part of the Fe/Nb diffusion couple annealed at 1300 °C. The zone with the eutectoid microstructure has formed by the eutectoid reaction δFe(Nb) ↔ γFe(Nb) + Fe_2Nb during cooling. Phases given in round brackets transformed during cooling

3.3 Fe_2Nb

EPMA results obtained from the two-phase alloys and the diffusion couple fit well to each other and together with recent EPMA measurements [1993bZel, 2005Tak, 2007Gru] they give a consistent set of data for the two intermetallic phases (Fig. 2). According to Fig. 2 the hexagonal C14-type Laves phase Fe_2Nb is stable between 25.1 (at 1373 °C) and 37.6 at.% Nb (1523 °C). This confirms earlier EPMA results, which already indicated that Fe_2Nb might have a considerable homogeneity range: 28.2-37.0 at.% Nb at 1200-1250 °C and 30.5-37 at.% Nb at 1350-1400 °C [1971aLei, 1971bLei], 27.5-35.5 at.% Nb at 1200 °C [2005Tak], 27.4-36.3 at.% Nb at 1100 °C [2007Gru] (supported by additional x-ray diffraction data in [1971aLei, 1971bLei, 2007Gru]), with the notable exception of Zelaya Bejarano et al. who gave 32-37 at.% Nb [1993bZel]. However, all assessments indicated much narrower homogeneity ranges: 32-37.5 [1982Kub], 33.3 [1990Hua], 32-37 [1994Sri, 1995Oka], 30-35 [2000Tof], with the exception of 27-38 at.% Nb [1986Pau].

The congruent melting temperature of Fe_2Nb established by DTA is 1646 ± 5 °C, which is well in the range of previously measured data; 1650-1660 [1938Egg], 1625 °C [1958Ell], 1627 ± 20 °C [1972Bew], 1630 °C [1991Zel,

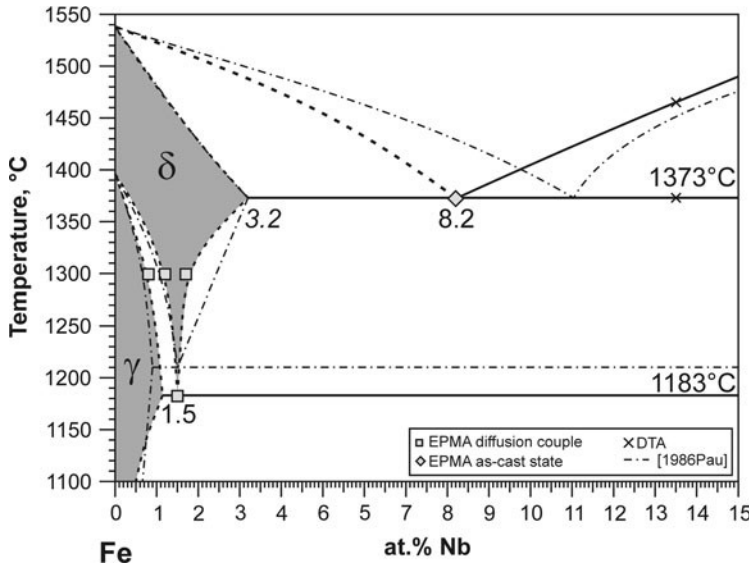

Fig. 5 Fe-rich part of the Fe-Nb system as obtained from the present EPMA and DTA data and compared to the assessment of [1986Pau]

1993bZel] or 1640 °C [1993aZel]. It is noted that even very close to the stoichiometric composition not a single effect is observed in the DTA (Table 2) as it would have been expected for a congruently melting phase. Instead a small shoulder is observed on the low-temperature side of heating and cooling peaks as is indicative of a still existing two-phase field $Fe_2Nb + L$. According to the recommendations by Boettinger et al. [2006Boe, 2007Boe], the solidus temperatures listed in Table 2 were always taken from the first deviation from the base line during heating and the liquidus temperatures were obtained in the same way from the cooling curves. In some cases there was indication of weak undercooling, e.g. when cooled with 10 K/min the alloy with 32.9 at.% Nb solidified about 10 K below the liquidus of alloys with similar composition. Ignoring the values affected by undercooling, the congruent melting temperature of Fe_2Nb was established by extrapolating the solidus and liquidus from both sides of the stoichiometric composition towards 33.3 at.% Nb.

3.4 Fe_7Nb_6

The μ phase Fe_7Nb_6, which forms by the peritectic reaction $L + Fe_2Nb \leftrightarrow Fe_7Nb_6$ at 1523 °C, has the hexagonal (rhombohedral) W_6Fe_7-type structure [1967Ram, 1968Kri]. According to Fig. 2, Fe_7Nb_6 is stable between 46.5-51.0 at.% Nb. This is within the range of previously established data, however the homogeneity range is somewhat broader than indicated by most previous reports: 47.5 to ~49.5 [1957Gol, 1960Gol], 47-49 [1967Ram], 48-50 [1968Kri], 49-50 [1971aLei], 48-52 at.% Nb [1993bZel]. There is no indication that the phase disintegrates below about 600 °C as claimed in [1957Gol, 1960Gol, 1975Kau, 1982Kub] and the phase boundaries are about vertical in the range of investigated temperatures and not inclined as shown in the latest assessments [2000Tof, 2002Oka, 2008Yos].

3.5 Nb-Rich Part

The maximum solubility for Fe in Nb is found at the invariant reaction $L \leftrightarrow Fe_7Nb_6 + Nb$ at 1508 °C. According to the present results (Fig. 2) the maximum solubility is about 9 at.% Fe, which is somewhat higher than previous data: ~5 at.% Fe [1960Gol], 7 at.% Fe [1993bZel] (however after 1500 °C/90 h they measure 8.8 at.% Fe by EPMA [1993aZel]), but in agreement with data established for lower temperatures which already indicated a higher solid solubility for Nb in Fe: ~7 at.% Fe at 1300 °C [1967Ram]. Values obtained by thermodynamic calculations scatter between about 5 and 9 at.% Fe [1975Kau, 1990Hua, 1994Sri, 2000Tof, 2008Yos].

4. Summary and Conclusions

The analysis of recent results obtained on the system Fe-Nb confirms that only two intermetallic phases exist, the hexagonal C14-type Fe_2Nb Laves phase which melts congruently at 1646 °C and the μ phase Fe_7Nb_6 which forms by the peritectic reaction $L + Fe_2Nb \leftrightarrow Fe_7Nb_6$ at 1523 °C. Both exist within a considerable range of compositions of about 12 and 5 at.% Nb, respectively. Both phase fields exhibit an asymmetric shape compared to their stoichiometric compositions, the Laves phase extending to the Fe-rich and the μ phase to the Fe-poor side. Based upon a data set of 13 single-phase Fe_2Nb alloys analysed by DTA the solidus and liquidus lines belonging to the Laves phase region are well described. The present investigation also adds up information on the Fe and Nb solid solutions. The eutectic compositions are determined as 8.2 ± 0.5 at.% Nb and 58.6 ± 0.7 at.% Nb and the eutectoid composition in the Fe-rich corner is confirmed to be 1.5 ± 0.1 at.% Nb. It is specifically noted that the present results fit to most of the previously reported experimental data. However, thermodynamic evaluations based on those results, of which several were conducted within the last 25 years, mostly fail to produce a proper phase diagram. Especially for the two intermetallic compounds, they all indicate homogeneity ranges which are quite different from the experimentally determined ones and they give markedly higher Nb contents for the eutectic composition of $L \leftrightarrow Fe_7Nb_6 + Nb$.

Acknowledgments

This work was carried out in the Inter-Institutional Research Initiative "The Nature of Laves Phases" funded by the Max Planck Society. The authors would like to thank Mrs. Irina Wossack for the EPMA measurements and Mr. Michael Kulse for sample preparation of the arc-melted samples.

References

1937Vor: N.M. Voronov, Alloys of Iron with Niobium, *Izv. Akad. Nauk SSSR, Otd. Mat. Estestv. Nauk*, 1937, p 1369-1379, in Russian

1938Egg: H. Eggers and W. Peter, The Iron-Niobium Phase Diagram, *Mitt. Kaiser Wilhelm Inst. Eisenforsch. Düsseldorf*, 1938, **20**(15), p 199-203, in German

1938Vog: R. Vogel and R. Ergang, The Iron-Niobium System, *Arch. Eisenhüttenwes.*, 1938, **12**(3), p 155-156, in German

1939Gen: R. Genders, Niobium-Iron alloys, *J. Iron Steel Inst.*, 1939, **140**, p 29-37

1942Wev: F. Wever and W. Peter, Precipitation and Age Hardening in Iron-Niobium Alloys and Niobium Steels, *Arch. Eisenhüttenwes.*, 1942, **15**(8), p 357-363, in German

1958Ell: J.F. Elliott and W. Rostoker, The Occurrence of Laves-type Phases Among Transition Elements, *Trans. ASM*, 1958, **50**, p 617-633

1957Gol: H.J. Goldschmidt, New Intermediate Phases in the Iron-Niobium System, *Research*, 1957, **10**, p 289-291

1960Gol: H.J. Goldschmidt, The Constitution of the Iron-Niobium-Silicon System, *J. Iron Steel Inst.*, 1960, **194**(2), p 169-180

1961Gib: W.S. Gibson, J.R. Lee, and W. Hume-Rothery, Liquidus-Solidus Relations in Iron-Rich Iron-Niobium and Iron-Molybdenum Alloys, *J. Iron Steel Inst.*, 1961, **198**(5), p 64-66

1964Fer: A. Ferrier, E. Übelacker, and E. Wachtel, Study of the Iron-Niobium Phase Diagram Between 0 and 12 at.% Nb from 1200-1535 °C, *C. R. Hebd. Séances Acad. Sci. (Paris)*, 1964, **258**, p 5424-5427, in French

1967Ram: A. Raman, Structural Study of Niobium-Iron Alloys, *Proc. Indian Acad. Sci. Sect. A*, 1967, **65**(4), p 256-264

1968Kri: P.I. Kripyakevich, E.I. Gladyshevskii, and R.V. Skolozdra, W6Fe7-Type Compounds in the Nb-Fe, Ta-Fe, and Ta-Co Systems, *Sov. Phys. Cryst.*, 1968, **12**(4), p 525-527

1970Fis: W.A. Fischer, K. Lorenz, H. Fabritius, and D. Schlegel, Investigation of the α/γ-Transformation in High-Purity Binary Alloys of Iron with Molybdenum, Vanadium, Tungsten, Niobium, Tantalum, Zirconium and Cobalt, *Arch. Eisenhüttenwes.*, 1970, **41**(5), p 489-498, in German

1971aLei: G. Leitner, "Investigations About Occurrence, Relationship and Variability of Some Lattice Types of Intermetallic Compounds," Ph.D. thesis, Fakultät für Naturwissenschaften und Mathematik, TU Dresden, 1971, p 1-205, in German

1971bLei: G. Leitner, Radius Ratio and Lattice Constants of Laves Phases, especially within the Homogeneity Range of $NbFe_2$, *Wiss. Z. Tech. Univ. Dresden*, 1971, **20**(2), p 391-394, in German

1972Bew: K. Bewilogua, R. Reichelt, K. Wetzig, and H. Wittig, Emission Electron Microscope Investigations of the Binary System Niobium-Iron, *Krist. Tech.*, 1972, **7**(5), p 601-609, in German

1975Kau: L. Kaufman and H. Nesor, Calculation of Superalloy Phase Diagrams: Part IV, *Metall. Trans.*, 1975, **6A**(11), p 2123-2131

1982Kub: O. Kubaschewski, Iron-Niobium, *Iron-Binary Phase Diagrams*, Springer-Verlag, Berlin & Verlag Stahleisen, Düsseldorf, 1982, p 70-73

1985Lue: F.X. Lü and K.H. Jack, The Occurrence of High-Speed Steel Carbide-Type η Phases in the Fe-Nb System, *J. Less-Common Met.*, 1985, **114**(1), p 123-127

1986Pau: E. Paul and L.J. Swartzendruber, The Fe-Nb System, *Bull. Alloy Phase Diagrams*, 1986, **7**(3), p 248-254

1990Hua: W. Huang, A Thermodynamic Evaluation of the Fe-Nb-C System, *Z. Metallkd.*, 1990, **81**(6), p 397-404

1991Zel: J. M. Zelaya Bejarano, S. Gama, C.A. Ribeiro, G. Effenberg, and C. Santos, On the Existence of the Fe_2Nb_3 Phase in the Fe-Nb System, *Z. Metallkd.*, 1991, **82**(8), p 615-620

1993Oka: H. Okamoto, Fe-Nb, *J. Phase Equilib.*, 1993, **14**(5), p 652-653

1993aZel: J.M. Zelaya Bejarano, "Investigation of the Ternary Diagram Iron-Aluminum-Niobium," Ph.D. thesis, Dept. of Materials Engineering, Universidade Estadual de Campinas, 1993, p 1-148, in Portuguese

1993bZel: J.M. Zelaya Bejarano, S. Gama, C.A. Ribeiro, and G. Effenberg, The Iron-Niobium Phase Diagram, *Z. Metallkd.*, 1993, **84**(3), p 160-164

1994Kai: R. Kainuma, M. Palm, and G. Inden, Solid-Phase Equilibria in the Ti-Rich Part of the Ti-Al System, *Intermetallics*, 1994, **2**(4), p 321-332

1994Sri: S. Srikanth and A. Petric, A Thermodynamic Evaluation of the Fe-Nb System, *Z. Metallkd.*, 1994. **85**(3), p 164-170

1995Oka: H. Okamoto, Comment on Fe-Nb, *J. Phase Equilib.*, 1995, **16**(4), p 369

1996Sch: C.G. Schön and J.A.S. Tenório, The Chemistry of the Iron-Niobium Intermetallics, *Intermetallics*, 1996, **4**(3), p 211-216

2000Tof: C. Toffolon and C. Servant, Thermodynamic Assessment of the Fe-Nb System, *CALPHAD*, 2000, **24**(2), p 97-112

2002Kne: V. Knezevic, G. Sauthoff, J. Vilk, G. Inden, A. Schneider, R. Agamennone, W. Blum, Y. Wang, A. Scholz, C. Berger, J. Ehlers, and L. Singheiser, Martensitic/Ferritic Super Heat-resistant 650 °C Steels-Design and Testing of Model Alloys, *ISIJ Int.*, 2002, **42**(12), p 1505-1514

2002Oka: H. Okamoto, Fe-Nb, *J. Phase Equilib.*, 2002, **23**(1), p 112

2005Fal: L. Falat, A. Schneider, G. Sauthoff, and G. Frommeyer, Mechanical Properties of Fe-Al-M-C (M = Ti, V, Nb, Ta) Alloys with Strengthening Carbides and Laves Phase, *Intermetallics*, 2005, **13**(12), p 1256-1262

2005Tak: M. Takeyama, N. Gomi, S. Morita, and T. Matsuo, Phase Equilibria and Lattice Parameters of Fe_2Nb Laves Phase in Fe-Ni-Nb Ternary System at Elevated Temperatures, *Mater. Res. Soc. Symp. Proc.*, 2005, **842**, p 461-466

2006Boe: W.J. Boettinger, U.R. Kattner, K.-W. Moon, and J.H. Perepezko, *DTA and Heat-Flux DSC Measurements of Alloy Melting and Freezing*, NIST Special Publication No. 960-15, 2006, p 1-90

2007Boe: W.J. Boettinger, U.R. Kattner, K.-W. Moon, and J.H. Perepezko, DTA and Heat-Flux DSC Measurements of Alloy Melting and Freezing, *Methods for Phase Diagram Determination,* J.-C. Zhao, Ed., Elsevier, Amsterdam, 2007, p 151-221

2007Gru: D. Grüner, *Investigation of the Nature of Laves Phases in the Systems with Transition Metals*, Fakultät Mathematik und Naturwissenschaften, Technische Universität Dresden, 2007, p 1-272 (online available at: http://nbn-resolving.de/urn:nbn:de:swb:14-1172078219643-48967), in German

2008Yam: Y. Yamamoto, M. Takeyama, Z.P. Lu, C.T. Liu, N.D. Evans, P.J. Maziasz, and M.P. Brady, Alloying Effects on Creep and Oxidation Resistance of Austenitic Stainless Steel Alloys Employing Intermetallic Precipitates, *Intermetallics*, 2008, **16**(3), p 453-462

2008Yos: K. Yoshitomi, Y. Nakama, H. Ohtani, and M. Hasebe, Thermodynamic Analysis of the Fe-Nb-B System, *ISIJ Int.*, 2008, **48**(6), p 835-844

2010Bal: S.K. Balam and A. Paul, Interdiffusion Study in the Fe-Nb System, *Metall. Mat. Trans. A*, 2010, **41A**(9), p 2175-2179

2010Vos: S. Voß, F. Stein, M. Palm, and D. Raabe, Synthesis of Defect-Free Single-Phase Bars of High-Melting Laves Phases Through Modified Cold Crucible Levitation Melting, *Mater. Sci. Eng. A*, 2010, **527**, p 7848–7853